Color Correction Using Root-Polynomial Regression

Graham D. Finlayson, *Member, IEEE*, Michal Mackiewicz, and Anya Hurlbert

***Abstract*— Cameras record three color responses (*RGB*) which are device dependent. Camera coordinates are mapped to a standard color space, such as XYZ—useful for color measurement—by a mapping function, e.g., the simple 3×3 linear transform (usually derived through regression). This mapping, which we will refer to as linear color correction (LCC), has been demonstrated to work well in the number of studies. However, it can map *RGB*s to XYZs with high error. The advantage of the LCC is that it is independent of camera exposure. An alternative and potentially more powerful method for color correction is polynomial color correction (PCC). Here, the *R*, *G*, and *B* values at a pixel are extended by the polynomial terms. For a given calibration training set PCC can significantly reduce the colorimetric error. However, the PCC fit depends on exposure, i.e., as exposure changes the vector of polynomial components is altered in a nonlinear way which results in hue and saturation shifts. This paper proposes a new polynomial-type regression loosely related to the idea of fractional polynomials which we call root-PCC (RPCC). Our idea is to take each term in a polynomial expansion and take its *k*th root of each *k*-degree term. It is easy to show terms defined in this way scale with exposure. RPCC is a simple (low complexity) extension of LCC. The experiments presented in this paper demonstrate that RPCC enhances color correction performance on real and synthetic data.**

***Index Terms*— Color correction, camera characterization, polynomial regression.**

I. Introduction

THE problem of colour correction arises from the fact that camera sensor sensitivities cannot be represented as the linear combination of CIE colour matching functions [1] (they violate the Luther conditions [2], [3]). The violation of the Luther conditions results in camera-eye metamerism [4] that is certain surfaces while different to the eye will induce the same camera responses and vice-versa. While colour correction cannot resolve metamerism per se, it aims at establishing the best possible mapping from camera RGBs to device independent XYZs (or display sRGBs [5]).

The literature is rich in descriptions of different methods attempting to establish the mapping between RGBs and XYZs. Methods include: 3D look-up tables [6], least-squares linear and polynomial regression [7]–[13] and neural networks [12], [14], [15].

Despite the variety of colour correction methods reported in the literature the simple 3×3 linear transform is not easily challenged. First, if we assume that reflectances can be represented by 3D linear model (approximately the case) [16], then under a given light the mapping from RGB to XYZ has to be a 3×3 matrix. Marimont and Wandell [17] extended the notion of modelling surface reflectances using linear models by proposing that a linear model should account only for that part of the reflectance which can be measured by a camera or a human eye or in general any set of sensors (under different lights). They found that typical lights and surfaces interact with typical cameras as if reflectances and illuminants were well described by the 3D linear models.

Another advantage of the linear colour correction (LCC) is that it works correctly as scene radiance/exposure changes. Let's assume that for a certain camera exposure setting, a surface in the scene represented by the RGB vector $\mathbf{v}$ is mapped to the XYZ vector $\mathbf{w}$. We would expect any colour correction algorithm to map $k\mathbf{v}$ to $k\mathbf{w}$ as well, where k denotes a scaling factor of the surface radiance (an additional assumption is that both $\mathbf{v}$ and $k\mathbf{v}$ are in the unsaturated range of the camera). This formal description is equivalent to having the same surface viewed under different light levels in different parts of the scene. The key observation here is that the LCC has this important property i.e. as surface radiance and so the RGBs are scaled up and down, the corresponding XYZ values will be scaled accordingly. In other words, the correct linear map taking RGBs to XYZs (or display sRGBs) is the same for both $\mathbf{v}$ and $k\mathbf{v}$. By a similar reasoning, LCC is also invariant to the changes in camera exposure settings.

Despite these benefits, LCC may produce significant errors for some surfaces. Indeed, given a linear fit from RGBs to XYZs, errors for individual surfaces can be in excess of 10 CIE ΔE ($1\Delta E$ denotes just noticeable difference [18], $10\Delta E$ differences are highly visually different).

To reduce this error a simple extension to the linear approach is to use polynomial colour correction (PCC) [7], [11]. In the 2^{nd} degree PCC each image RGB is represented by the 9-vector $[R\ G\ B\ R^2\ G^2\ B^2\ RG\ RB\ GB]$. Analogously, one can define a higher degree polynomials e.g. the 3^{rd} degree where the RGB vector is extended to 19 elements and the 4^{th} degree where it is extended to 34 elements. Significantly, a polynomial fit can - for fixed calibration settings - reduce the mapping error (even in excess of 50%) [11]. Unfortunately, if the RGB is scaled by k, the individual components of the 9-vector either scale by k or k^2. Thus, if we scale our data - physically this is the effect of changing the scene radiance

Manuscript received January 4, 2013; revised January 2, 2015; accepted February 2, 2015. Date of publication February 24, 2015; date of current version March 6, 2015. This work was supported by the U.K. Engineering and Physical Sciences Research Council under Grant EP/H022236/1 and Grant EP/H022325/1. The associate editor coordinating the review of this manuscript and approving it for publication was Prof. Vishal Monga.

G. D. Finlayson and M. Mackiewicz are with the School of Computing Sciences, University of East Anglia, Norwich NR4 7TJ, U.K. (e-mail: g.finlayson@uea.ac.uk; m.mackiewicz@uea.ac.uk).

A. Hurlbert is with the Institute of Neuroscience, Newcastle University, Newcastle upon Tyne NE1 7RU, U.K. (e-mail: anya.hurlbert@newcastle.ac.uk).

Color versions of one or more of the figures in this paper are available online at http://ieeexplore.ieee.org.

Digital Object Identifier 10.1109/TIP.2015.2405336

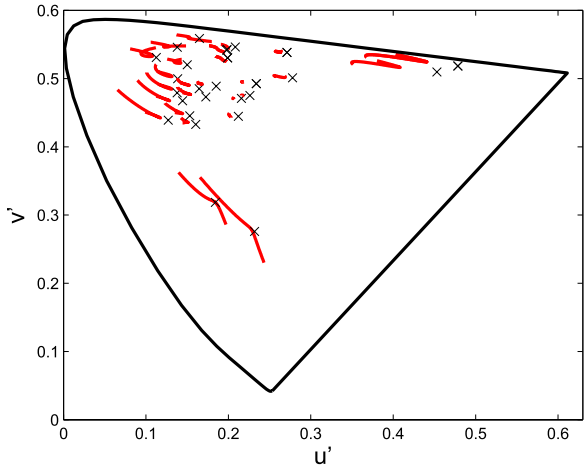

Fig. 1. Selection of reflectances from the SFU 1995 dataset [19] and their true $u'v'$ coordinates (x) [18]; chromatic shifts produced by the polynomial model of the 4^{th} degree (red solid lines).

or exposure - then the best 3×9 colour correction matrix must also change. This presents a significant problem in real images.

Fig. 1 illustrates the problem. We map the scene physical colours at a number of exposures using PCC and plot the corresponding chromaticities. One can clearly see the chromatic shifts induced by the PCC as one scales the intensity of the light. The red lines show that the scene physical input chromaticity might be mapped to a range of outputs depending on exposure.

A real image example of the problem is presented in Fig. 2. Fig. 2a contains an image of the colour checker captured with the NIKON D70 camera and colour corrected with the polynomial model of the 4^{th} degree. Fig. 2b shows the same image with double the exposure time before it was corrected by the same transform. One can see that the colours of some patches have changed as the exposure changed e.g. an orange patch is corrected to pink as exposure changes.

Other examples of PCC failure are shown in Fig. 3. The scene containing the Macbeth colour chart and a pepper fruit under the D65 illuminant was captured with the Specim VNIR hyperspectral camera[1] and integrated with the sRGB sensors (shown in Fig. 3a). Next, the scene was integrated with Foveon sensors [20] and colour corrected by the 4^{th} degree PCC (shown in Fig. 3b). This image shows a relatively good colour correction when compared with the sRGB image. However, when we look at the image that was colour corrected after the illumination level was increased (shown in Fig. 3c), we can see that some colours were rendered inaccurately (e.g. the cyan patch and the pepper highlight). Note, that these patches are still below the sensor saturation level (the white point in the original image).

In this paper, we develop a new Root Polynomial Colour Correction (RPCC). By taking the k^{th} root of k-degree polynomial terms, we show RPCC is independent of exposure (like LCC).

[1]www.specim.fi

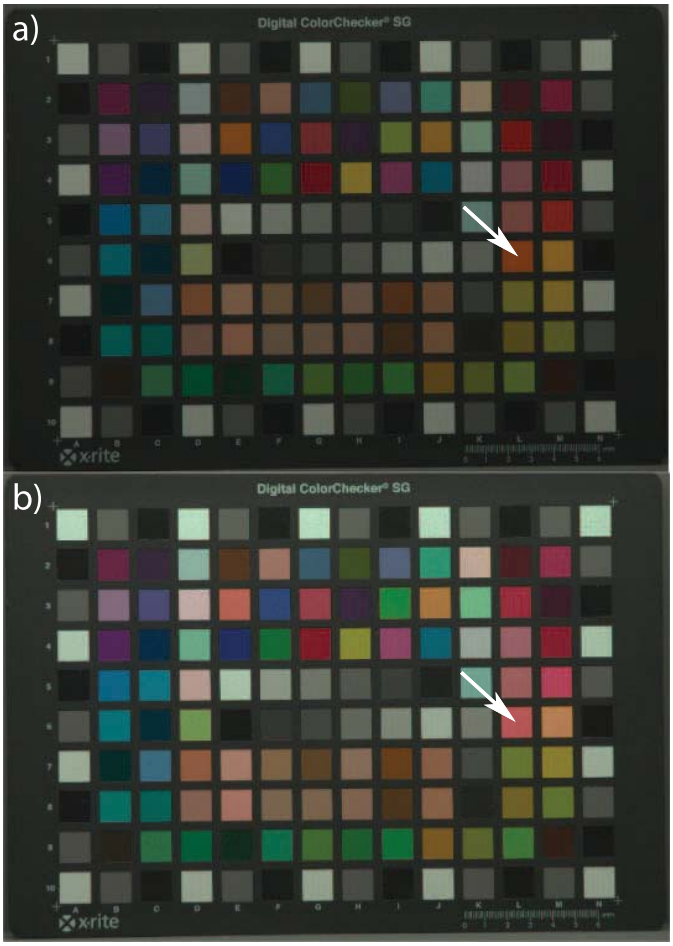

Fig. 2. X-rite SG colour chart captured with NIKON D70 camera and colour corrected using the polynomial model of the 4^{th} degree (a). The image RGB values were multiplied by 2 before applying the same colour correction transform (b). A sample pair of patches with high error has been marked with arrows.

The rest of the paper is organised as follows. In Section II, we describe the PCC and a few other alterations to the LCC. In Section III, we set out our root-polynomial method. This is followed by the experiments in Section IV, discussion in Section V and conclusions in Section VI.

II. Polynomial Colour Correction

Let $\boldsymbol{\rho}$ define a three element vector representing the three camera responses and $\mathbf{q}$ their corresponding tristimulus values. A simple 3×3 colour correction transform is written as:

$$\mathbf{q} = \mathbf{M}\boldsymbol{\rho} \tag{1}$$

The matrix $\mathbf{M}$ is generally found by some sort of least-squares regression. Let us denote a set of N known XYZs for a reflectance target as $\mathbf{Q}$ and the corresponding camera responses as the $3 \times N$ matrix $\mathbf{R}$. We find the least-squares mapping from $\mathbf{R}$ to $\mathbf{Q}$ using the Moore-Penrose inverse [21]:

$$\mathbf{M} = \mathbf{Q}\mathbf{R}^T(\mathbf{R}\mathbf{R}^T)^{-1} \tag{2}$$

In polynomial regression, vector $\boldsymbol{\rho}$ is extended by adding additional polynomial terms of increasing degree. Formally, let $\boldsymbol{\rho}$ denote responses from N sensors. Then, the set of up to

Fig. 3. The scene containing the Macbeth colour chart and a pepper fruit illuminated with D65 metamer, captured with Specim hyperspectral camera and integrated with the sRGB sensors (a). The same hyperspectral image, integrated with Foveon sensors and colour corrected to sRGB using the polynomial model of the 4^{th} degree (b). The same colour correction performed after the intensity of the light was increased by 70% (c).

K^{th} degree polynomial terms in N variables is defined as:

$$P_{K,N} = \left\{ \boldsymbol{\rho}^{\alpha} : |\alpha| \leq K \right\} \tag{3}$$

where $\alpha = (\alpha_1, ..., \alpha_N)^T$ is a *multi-index* that is n-tuple of non-negative integers and its size is defined as $|\alpha| = \alpha_1 + ... + \alpha_N$ [22]. In multi-index notation, $\boldsymbol{\rho}^{\alpha} = \prod_{i=1}^{N} \rho_i^{\alpha_i}$. There are $\left(\left(\frac{N}{K}\right)\right) = \binom{N+K-1}{N-1} = \binom{N+K-1}{K}$ different multi-indices of size K [23], and so, that many polynomial terms of degree K. It can be shown that the number of polynomials of up to K^{th} degree in N variables is $h = \binom{N+K}{N} - 1 = \binom{N+K}{K} - 1$.

For a typical case when $N = 3$ i.e. $\boldsymbol{\rho} = (r, g, b)^T$, the polynomial expansions of the 2^{nd}, 3^{rd} and 4^{th} degree investigated in this work are given by the sets $P_{2,3}$, $P_{3,3}$ and $P_{4,3}$, which after ordering are defined by the following vectors:

$$\begin{aligned}
\boldsymbol{\rho}_{2,3} &= \left(r, g, b, r^2, g^2, b^2, rg, gb, rb\right)^T \\
\boldsymbol{\rho}_{3,3} &= \left(r, g, b, r^2, g^2, b^2, rg, gb, rb,\right. \\
&\qquad \left. r^3, g^3, b^3, rg^2, gb^2, rb^2, gr^2, bg^2, br^2, rgb\right)^T \\
\boldsymbol{\rho}_{4,3} &= \left(r, g, b, r^2, g^2, b^2, rg, gb, rb,\right. \\
&\qquad r^3, g^3, b^3, rg^2, gb^2, rb^2, gr^2, bg^2, br^2, rgb, \\
&\qquad r^4, g^4, b^4, r^3g, r^3b, g^3r, g^3b, b^3r, b^3g, \\
&\qquad \left. r^2g^2, g^2b^2, r^2b^2, r^2gb, g^2rb, b^2rg\right)^T
\end{aligned}$$

In a polynomial expansion the 3 numbers recorded in a pixel are represented by 9, 19 and 34 numbers respectively. Colour correction is now carried out by 3×9, 3×19 and 3×34 matrices. If $\mathbf{R}$, in general, denotes the polynomial response of N surfaces then Equation 2 can be used to solve for the PCC matrix. Of course high degree data expansions can result in unstable (rank deficient) data sets. This problem can be mitigated by regularising the regression [21], [24].

LCC has been extracted in a variety of different ways. In [25] Vrhel and Trussel showed that if the mapping is defined relative to the first three principal components of the training set of surface reflectances then relatively good colour correction is often obtained for the entire set. Finlayson and Drew [10] proposed a constrained least-squares regression, where the 3×3 linear transform is constrained to map one (or possibly 2) colour patches exactly. The authors call this transform the white preserving colour correction (WPCC). In 3×3 LCC, preserving one colour leaves two degrees of freedom to be determined by the least-squares fit. Similarly, preserving two colours leaves one degree of freedom to be determined by the least-squares fit and preserving three colours fully determines the colour correction matrix. The authors observed that it is often beneficial to have the white-point preserving mapping which can be achieved within the framework of their method. Constrained regression is particularly useful when there is incomplete training set in which case a so called *maximum ignorance* training is often performed. This method is also applicable using a polynomial expansion of R, G and B.

Andersen and Hardeberg proposed the Hue Plane Preserving Colour Correction (HPPCC) [26], which maps RGBs to XYZs using a finite (on the order of a dozen) set of linear transforms, where each transform is applied in a different hue slice of the colour space. Thus, in general different pixels are corrected using different 3×3 linear transforms. Each individual 3×3 transform M_i is derived only from 3 patches: a neutral and two chromatic patches specifying the extent of the hue slice. This ensures the error free mapping of the three patches and the C0 continuity of the XYZ estimates at the hue slice boundaries. The authors show that their method outperforms both the basic LCC as well as the WPCC mentioned above. It also outperforms the 2^{nd} degree PCC. Further, the authors point out that unlike the other three methods, the PCC will not preserve hue planes across different exposures. A target such as the Macbeth colour chart (19 distinct chromaticities) does not have sufficient colour diversity to train this method.

Other variations of LCC include deriving transforms aiming to be robust to noise [13], [27].

III. Root-Polynomial Colour Correction

For fixed exposure, polynomial regression really can deliver significant improvements to colour correction. However, in reality the same reflectance will also induce many different brightnesses for the same fixed exposure and viewing conditions. As an example, due to shading the same physical reflectance might induce camera responses from zero to the maximum sensor value. Clearly, for this circumstance we want the colour of the object (hue and saturation) to be constant throughout the brightness range. As shown in Fig. 1-3 simple polynomial regression does not preserve object colour.

The starting point of this paper was to ask the following question. Is there a way we can use the undoubted power of polynomial data fitting in a way that does not depend on exposure/scene radiance? We make the observation that the terms in any polynomial fit each have a degree e.g. R, RG and R^2B are respectively degree 1, 2 and 3. Multiplying each of R, G and B by a scalar k results in the terms kR, k^2RG and k^3R^2B. That is the degree of the term is reflected in the power to which the exposure scaling is raised. Clearly, and this is our key insight, taking the degree-root will result in terms which have the same k scalar: $(kR)^{1/1} = kR$, $(k^2RG)^{1/2} = k(RG)^{1/2}$, $(k^3R^2B)^{1/3} = k(R^2B)^{1/3}$. For a given p^{th} degree polynomial expansion, we take each term and raise it to the inverse of its degree. The unique individual terms that are left are what we use in Root-Polynomial Colour Correction.

Formally, the set of up to K^{th} degree root-polynomial terms in N variables is defined as:

$$\overline{P}_{K,N} = \left\{ \boldsymbol{\rho}^{\frac{\alpha}{|\alpha|}} : |\alpha| \leq K \right\}$$

Strictly speaking all root-polynomial terms are multi-variable polynomials (monomials) of degree 1 as we took the p^{th} root of every p^{th} degree polynomial term.

For a familiar RGB case when $N = 3$ i.e. $\boldsymbol{\rho} = (r, g, b)^T$, the root-polynomial expansions of the 2^{nd}, 3^{rd} and 4^{th} degree are given below:

$$\overline{\boldsymbol{\rho}}_{2,3} = \left(r, g, b, \sqrt{rg}, \sqrt{gb}, \sqrt{rb}\right)^T$$

$$\overline{\boldsymbol{\rho}}_{3,3} = \left(r, g, b, \sqrt{rg}, \sqrt{gb}, \sqrt{rb}, \sqrt[3]{rg^2}, \sqrt[3]{gb^2}, \sqrt[3]{rb^2}, \sqrt[3]{gr^2}, \sqrt[3]{bg^2}, \sqrt[3]{br^2}, \sqrt[3]{rgb}\right)^T$$

$$\overline{\boldsymbol{\rho}}_{4,3} = \left(r, g, b, \sqrt{rg}, \sqrt{gb}, \sqrt{rb}, \sqrt[3]{rg^2}, \sqrt[3]{gb^2}, \sqrt[3]{rb^2}, \sqrt[3]{gr^2}, \sqrt[3]{bg^2}, \sqrt[3]{br^2}, \sqrt[3]{rgb}, \sqrt[4]{r^3g}, \sqrt[4]{r^3b}, \sqrt[4]{g^3r}, \sqrt[4]{g^3b}, \sqrt[4]{b^3r}, \sqrt[4]{b^3g}, \sqrt[4]{r^2gb}, \sqrt[4]{g^2rb}, \sqrt[4]{b^2rg}\right)^T$$

Notice that the number of root-polynomial terms is reduced comparing to the number of polynomial terms - it is now smaller than h. This is because the root operation is many to 1. For example R, R^2, R^3 and their respective 1^{st}, 2^{nd} and 3^{rd} roots are all equal to R. Similarly RG, R^2G^2, R^3G^3 and their respective 2^{nd}, 4^{th} and 6^{th} roots are all equal to $\sqrt{RG}$. Clearly R or $\sqrt{RG}$ can only occur once in the root polynomial regression. Thus, colour correction is now carried out by 3×6, 3×13 and 3×22 matrices.

In Fig. 4, we can compare visually the two corresponding families of polynomial and root-polynomial functions for the simplest case case when $K = 2$ and $N = 2$ i.e. $\boldsymbol{\rho}_{2,2} = \left(r, g, r^2, g^2, rg\right)^T$ and $\overline{\boldsymbol{\rho}}_{2,2} = \left(r, g, \sqrt{rg}\right)^T$.

What we expect from the root-polynomial model is improvement over the linear model for the regions where linearity is poor (due to the types of surfaces, sensors and lights), but also, crucially, elimination of the effects of non-linear magnification of linear changes in the overall light level.

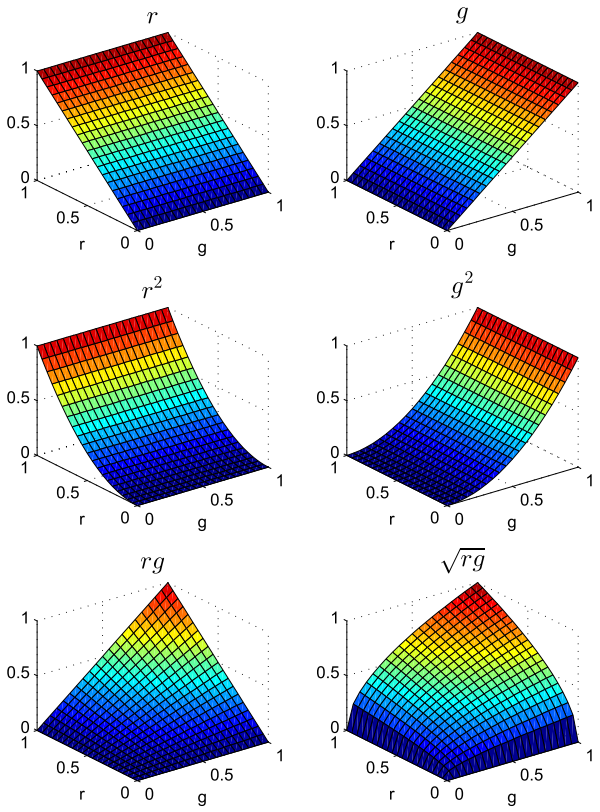

Fig. 4. Polynomial and root-polynomial basis functions from $P_{2,2}$ and $\overline{P}_{2,2}$ sets.

A. Theoretical Properties of Root-Polynomial Colour Correction

While experiments later in this paper will show that, empirically, RPCC works well - it delivers comparable or better colour correction compared with antecedent methods when exposure is fixed and better performance when it varies - we need to convince ourselves that the method is robust and will work well in general. The strength of normal polynomial regression lies on two important theoretical results. First, all the terms in a K^{th} degree polynomial expansion are linearly independent and so, plausibly, add new useful information to the regression. Second, that a $K + 1$ degree polynomial expansion always has more terms than a K^{th} degree expansion: we can, at least in principle, fit ever more complex functions simply by adding more higher degree terms.

This second result is particularly useful in the discrete domain where regressions are typically performed. If data is represented by a vector $\underline{X}$ of m unique measurements then an m-degree polynomial expansion of $\underline{X}$ will span m-dimensional space and so $\underline{X}$ can be related to any other variable, say $\underline{Y}$ by polynomial regression.

Below we prove two companion propositions for root-polynomial colour correction. We show that a K^{th} degree root polynomial basis is a basis. Second, that a $K + 1$ degree root-polynomial expansion adds more linearly independent terms. In the limit the root-polynomial expansion can, like conventional polynomial regression, provide a basis for any m dimensional vector space.

Let $\mathbb{V}$ be a real vector space generated by the set of root-polynomials $\overline{P}_{K,N}$.

Proposition 1: Elements of $\overline{P}_{K,N}$ are linearly independent and hence form a basis of $\mathbb{V}$.

Proof: We prove the above assuming $N = 2$ (2 sensors) and $K = 3$ (3^{rd} degree root-polynomial expansion). Our arguments naturally extend to higher number of sensors and higher degree expansions.

We denote the 2 sensors as r and g. The 1^{st} degree polynomial basis is simply the 2D coordinates themselves: r and g (where it is understood that that r and g can take on arbitrary values in the range 0 to 1). The 2^{nd} degree polynomial basis is denoted as r, g, r^2, g^2 and rg. The 3^{rd} degree polynomial basis has the additional terms r^3, g^3, r^2g and g^2r i.e.

$$P_{3,2} = \left\{r, g, r^2, g^2, rg, r^3, g^3, r^2g, g^2r\right\} \tag{4}$$

The root-polynomial expansion corresponding to the aforementioned 3^{rd} degree polynomial expansion is equal to:

$$\overline{P}_{3,2} = \left\{r, g, \sqrt{rg}, \sqrt[3]{r^2g}, \sqrt[3]{gr^2}\right\} \tag{5}$$

We notice that $\overline{P}_{3,2}$ has only 5 elements compared to 9 for the 3^{rd} degree polynomial $P_{3,2}$.

Let $r = \hat{r}^l$ and $g = \hat{g}^l$ (l is chosen so that the corresponding root powers become positive integers). Note that for $\overline{P}_{3,2}$, $l = 6$ i.e. $r = \hat{r}^6$ and $g = \hat{g}^6$. This substitution yields $\overline{P}_{3,2} \Leftrightarrow \hat{P}$ where

$$\hat{P} = \left\{\hat{r}^6, \hat{g}^6, \hat{r}^3\hat{g}^3, \hat{r}^2\hat{g}^4, \hat{g}^2\hat{r}^4\right\} \tag{6}$$

$\hat{P}$ is a set of 6^{th} degree unique polynomials and hence its elements are linearly independent. Thus, $\overline{P}_{3,2}$ (and in general $\overline{P}_{K,N}$) elements are also linearly independent and form a basis of $\mathbb{V}$. ∎

Proposition 2: $\overline{P}_{K+1,N}$ has more linearly independent elements than $\overline{P}_{K,N}$.

Proof: Suppose the K^{th} degree root-polynomial set has n elements. If K is even, then the K^{th} root-polynomial set has the term $r^{\frac{K}{2}-1}g^{\frac{K}{2}+1}$. If K is odd, then the K^{th} root-polynomial set has the term $r^{\frac{K-1}{K}}g^{\frac{1}{K}}$. Both terms cannot appear in any $L < K$ degree expansion as their corresponding fractional powers are in their simplest form. From Proposition 1 this new term contributes information to the basis expansion. ∎

Finally we would like to draw the readers' attention to Fig. 4 (bottom right). We can see that the surface of the $\sqrt{rg}$ function is relatively flat in the neighbourhood of the achromatic line. Similarly, the surfaces of higher degree root-polynomials e.g. $\sqrt[3]{r^2g}$, $\sqrt[3]{rg^2}$, $\sqrt[4]{r^3g}$ etc. are also relatively flat in this neighbourhood (in addition, they all intersect at the achromatic line) and will only have the steeper slopes closer to the rg-axes. This inherent property of the root-polynomial terms ensures root-polynomial regression tends to correctly preserve colors that are achromatic. The only way to achieve non-smooth data fits near the achromatic axis is when the coefficient vectors (deterring the fit) have large positive and negative values. Typically, our root-polynomial regression is regularized and this effectively limits the norm of the coefficient vector [21]. This is an important observation since many studies (see [28]) have shown that real-world objects, statistically, are desaturated. Colours which are very saturated are rare.

B. Related Work

Our proposition of root-polynomials is related to the fractional polynomials (termed by Royston and Altman in [29]; for more comprehensive review see [30]) being an extension of the BoxTidwell power transformation [31]. Using fractional exponents in polynomial fitting is common in statistics, but we are unaware of previous work that forms these specific polynomial terms which have the advantage that they all have degree 1. Royston and Altman noted that polynomial regression lacks in terms of the number of shapes for the low degree polynomials and is often unstable at the extreme values for the high degree polynomials (Runge's phenomenon). The authors suggested choosing the powers of the fractional polynomials from the following restricted set: $\{-2, -1, -0.5, 0, 0.5, 1, 2, 3\}$. In their notation, 'zero' power denotes $ln(x)$. Note, that the last three elements are the 'standard' polynomial powers. The authors applied their fractional polynomial models in medical data analysis. They concluded that using the extended set of polynomial powers offers more flexibility in fitting regression models to the data. The root-polynomials discussed here are not fractional polynomials in the strict sense as they all have degree 1. However, for all terms except the first three linear, the individual variables are in the fractional powers. The root-polynomials are also related to the multi-linear polynomials, which arise in a multi-linear LUT interpolation [32]. However, the latter do not have the desired property of degree 1 and hence will not demonstrate the aforementioned exposure invariance.

IV. Experiments

To measure the performance of the RPCC, we performed both real camera experiment and synthetic data simulations, which are given in the following subsections. For both types of data, we compared the performance of RPCC with the LCC and PCC up to degree of four. We also compared the above with the colour correction using the tri-linear LUT interpolation implemented as suggested in [32]. Here, we used $13\times13\times13$ LUT and employed the Graph Hessian Regularizer also described in the above reference. And finally, we tested the HPPCC [26] that was briefly described in Section II. As suggested by the authors, we partitioned the hue circle into twelve slices and performed sample selection based on relative susceptibility to noise (details of this procedure can be found in [26]).

A. Real Camera Experiments

We performed two real camera characterisations. The experimental set-up was as follows. The X-rite SG colour chart was positioned in a viewing box, illuminated with a D65 metamer [18] produced by

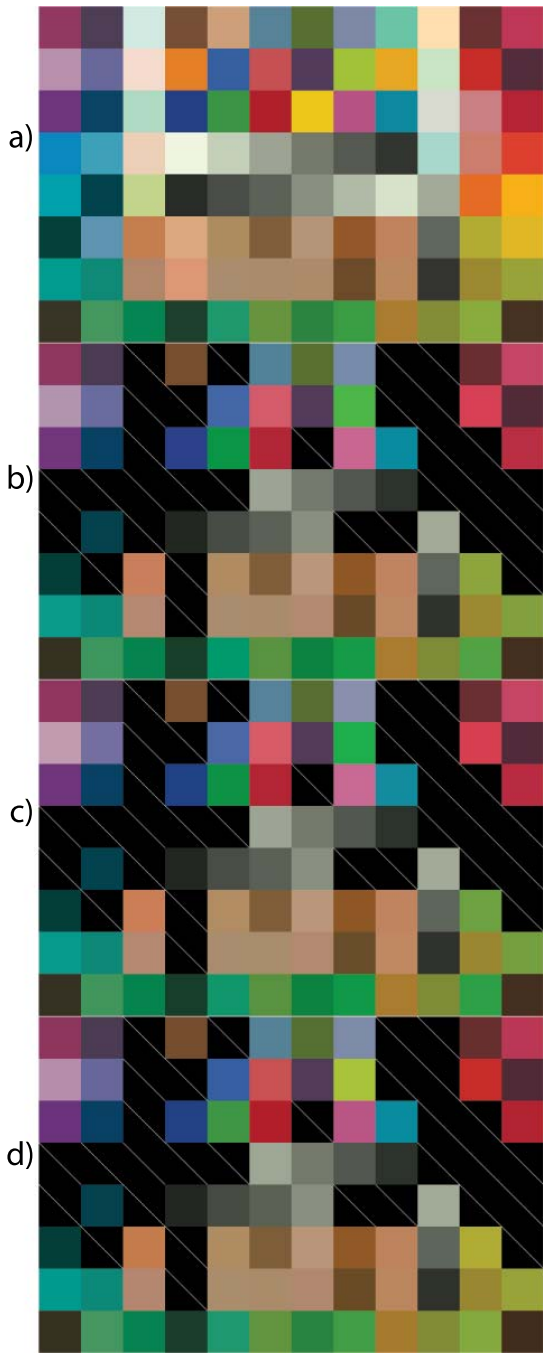

Fig. 5. SG chart synthesised from the spectrophotometer measurements (a). SG chart patches (66) captured with Nikon D70, multiplied by 2 and corrected with **polynomial of degree 3** (b), **degree 4** (c) and **root-polynomial of degree 4** (d). The patches that are crossed over have been removed as they were clipped following the multiplication. Note, these are synthetic patches derived from RGB averages.

Gamma Scientific RS-5B LED illuminator [33] and imaged with Nikon D70 and Sigma SD15 cameras. We also measured XYZs of each of the 96 patches using a Photo Research PR-650 spectrophotometer (see Fig. 5a). The linear 16-bit images were extracted from the camera raw images using DCRAW[2] (Nikon) and PROXEL X3F[3] (Sigma) packages.

[2]http://www.cybercom.net/~dcoffin/dcraw/
[3]http://www.proxel.se/x3f.html

The 96 patches were manually segmented and for the purpose of this exercise we used the average RGB of each patch. The dark levels were captured with the lens cap on and subtracted from the average camera responses [19]. Resulting RGBs and measured XYZs were used to derive a set of colour correction models as described in the earlier sections. The models were evaluated using the leave-one-out method i.e. we built the model using all but one of the surfaces from the dataset and tested that model on the remaining patch; we repeated this for all the patches in the dataset and calculated mean ΔE in the CIELUV colour space [18]. The results of the validation can be seen in the second column (original exposure) in Table I.

The remaining two columns contain the results of performing colour correction on the same image data after multiplying all RGBs by the factors of $\frac{1}{2}$ and 2 and excluding those patches whose at least one sensor response (R, G or B) exceeded the corresponding sensor response of the white patch at the original exposure. This ensures that we are not taking into account those patches which in the real situation would be clipped. Thus, after multiplying RGBs by the factor of 2, we are left with 66 out of the original 96 patches for the Nikon camera and with 73 patches for the Sigma camera (see the last rows of Table I).

Fig. 5a-d allow us to compare the colour correction errors visually. Fig. 5a contains the sRGB SG chart patches, whereas the remaining figures contain the patches that were synthesised from the manually segmented average Nikon D70 RGBs that were multiplied by 2 (simulating light intensity increase) and colour corrected using PCC of degree 3 (Fig. 5b), 4 (Fig. 5c) and RPCC of degree 4 (Fig. 5d). These figures correspond to the errors reported in Table I in column *multiplied by 2*. It can be clearly seen that as Table I suggests, the errors for the PCC of degree 3 and 4 are significant, which is particularly visible for some green as well as pink and red patches. In contrast the high degree RPCC result in Fig. 5d does not manifest these chromatic errors.

Table I shows that the RPCC performs better than the LCC and is invariant with respect to the change of illumination intensity. It is also clear that PCC fails under the change of illumination condition. The smaller errors for the Nikon sensors than those for the Sigma suggest that the former are more colorimetric than the latter. The LUT method provides comparable performance to the PCC, i.e. it outperforms the LCC for the original exposure, but is not exposure invariant so it is clearly worse than RPCC as the exposure level is varied. Against our expectations, HPPCC does not provide clearly better results than the LCC.

B. Synthetic Data Experiments

Here, we used the Sony DXC-930 camera [19] and Foveon sensor sensitivities [20] to integrate the spectral data from three surface reflectance datasets. The first dataset comprised 96 reflectances of the X-rite SG colour chart (border patches excluded), the second 180 patches of the Macbeth DC chart (again border patches excluded) and the third 1995 surfaces collated at the Simon Fraser University [19].

TABLE I

NIKON D70 AND SIGMA SD15 CHARACTERISATION RESULTS. THE ERRORS OBTAINED ARE GIVEN AS THE MEAN, MEDIAN AND 95 PERCENTILE ERROR IN THE CIELUV COLOUR SPACE

exposure	original exp.			divided by 2			multiplied by 2		
model type ($N = 3$)	mean	med	95 pt.	mean	med	95 pt.	mean	med	95 pt.
Nikon D70									
PCC,1 (LCC)	2.5	2.3	5.1	2.5	2.3	5.1	2.9	2.7	5.7
PCC,2	2.1	1.8	4.8	2.3	2.1	5.3	2.3	2.0	5.0
PCC,3	1.7	1.6	3.1	2.1	1.8	4.4	5.7	2.5	23
PCC,4	**1.6**	1.5	3.5	2.1	1.8	4.9	7.5	2.0	29
LUT	1.7	1.4	4.4	2.6	2.1	6.1	2.3	1.8	5.6
RPCC,2	1.9	1.7	4.0	1.9	1.7	4.0	2.1	1.8	3.8
RPCC,3	**1.6**	**1.3**	3.4	**1.6**	**1.3**	3.4	**1.8**	1.8	3.3
RPCC,4	**1.6**	1.4	**3.3**	**1.6**	1.4	**3.3**	**1.8**	**1.7**	**3.2**
HPPCC	2.5	2.1	6.0	2.5	2.4	6.0	2.6	2.4	5.9
number of patches	all (96)			all (96)			66		
Sigma SD15									
PCC,1 (LCC)	5.2	4.0	16	5.2	4.0	16	5.8	4.6	16
PCC,2	3.9	3.2	9.4	4.5	3.7	10	5.0	3.4	13
PCC,3	**3.1**	**2.3**	**7.0**	4.2	3.2	11	7.2	3.7	26
PCC,4	3.2	2.5	7.8	3.7	2.8	9.0	57	6.4	280
LUT	4.3	3.3	12	6.9	5.5	17	5.5	3.5	20
RPCC,2	3.8	2.8	8.7	3.8	2.8	8.7	4.1	2.9	9.6
RPCC,3	3.2	2.4	9.1	**3.2**	**2.4**	9.1	3.6	**2.6**	**9.3**
RPCC,4	3.2	2.5	8.6	**3.2**	2.5	**8.6**	**3.5**	2.7	9.4
HPPCC	5.0	3.2	17	5.0	3.2	17	5.7	3.4	18
number of patches	all (96)			all (96)			73		

TABLE II

SYNTHETIC DATA SIMULATION RESULTS FOR FIXED ILLUMINATION CONDITION

dataset	SG			DC			SFU		
model type ($N = 3$)	mean	med	95 pt.	mean	med	95 pt.	mean	med	95 pt.
Sony									
PCC,1 (LCC)	4.8	2.9	20	3.8	1.9	14	2.6	1.4	7.7
PCC,2	4.0	2.7	11	3.1	1.8	10	2.4	1.4	7.2
PCC,3	3.2	2.2	7.5	2.4	1.3	7.7	1.9	1.2	6.5
PCC,4	3.1	2.2	8.2	2.0	1.2	6.9	1.8	1.1	6.0
LUT	2.7	1.9	**7.3**	**1.8**	**1.0**	**6.7**	**1.5**	**1.0**	**5.0**
RPCC,2	2.8	1.8	8.7	2.4	1.3	8.5	2.1	1.2	7.0
RPCC,3	**2.6**	**1.6**	8.1	2.2	1.3	7.5	1.8	1.2	6.1
RPCC,4	**2.6**	**1.6**	8.3	2.2	1.3	7.7	1.8	1.1	6.1
HPPCC	3.8	2.2	14	2.8	1.4	10	3.6	1.8	14
Foveon									
PCC,1 (LCC)	3.9	3.6	10	3.6	2.5	10	2.5	1.6	7.5
PCC,2	2.9	2.4	6.8	2.9	2.2	8.6	2.2	1.7	5.7
PCC,3	2.2	1.6	5.8	2.1	1.6	6.3	1.9	1.5	5.0
PCC,4	2.5	1.7	7.5	**1.8**	**1.4**	**5.5**	**1.7**	**1.2**	**4.1**
LUT	3.4	2.7	9.9	2.7	1.7	8.7	2.0	1.4	5.2
RPCC,2	3.0	2.3	7.1	2.9	1.8	7.0	2.0	1.4	5.5
RPCC,3	**2.0**	**1.6**	**5.1**	2.2	1.4	6.4	1.9	1.4	5.0
RPCC,4	2.2	1.6	6.2	2.2	1.4	6.4	1.9	1.4	4.9
HPPCC	4.9	2.7	19	5.4	3.4	18	3.3	2.2	9.2

For each dataset we performed a simulation, in which we integrated both sensor sensitivities and the colour matching functions under D65 illuminant producing corresponding sets of camera responses (RGBs) and XYZs. Spectra calculations were carried out for 31 spectral channels - 400-700nm sampled every 10nm. Next, we built the previously described regression models. For each of the three datasets, we performed the leave-one-out validation in the same manner as in the earlier real camera experiments. We split the results and discussions of these simulations into four parts, which are given in the following four subsections.

1) Fixed Exposure: Table II synthetic data results correspond to the real camera results contained in the *original exp.* column in Table I. We can see that the RPCC usually performs similarly to the PCC of higher degree. However, it clearly outperforms the LCC. We can also see that for

TABLE III
SYNTHETIC DATA SIMULATION RESULTS FOR THE DC AND SFU DATASET AS THE LIGHT LEVEL WAS DECREASED AND INCREASED

dataset	DC divided by 2			DC multiplied by 2			SFU divided by 2			SFU multiplied by 2		
model type ($N = 3$)	mean	med	95 pt.	mean	med	95 pt.	mean	med	95 pt.	mean	med	95 pt.
Sony												
PCC,1 (LCC)	3.8	1.9	14	4.5	2.1	21	2.6	1.4	7.7	2.9	1.4	9.3
PCC,2	3.9	2.5	12	3.8	2.2	14	2.6	1.6	8.0	2.6	1.4	8.7
PCC,3	3.3	1.9	10	3.0	1.3	14	2.5	1.5	7.8	2.5	1.3	9.6
PCC,4	3.0	1.6	11	2.6	1.5	9.5	2.4	1.4	8.0	2.5	1.2	9.3
LUT	3.0	1.7	9.0	**2.3**	**1.2**	**9.3**	2.5	1.8	7.3	2.2	1.2	8.1
RPCC,2	2.4	**1.3**	8.5	2.6	1.4	**9.3**	2.1	1.2	7.0	2.2	1.2	7.5
RPCC,3	**2.2**	**1.3**	**7.5**	2.4	1.3	9.5	**1.8**	1.2	**6.1**	2.0	1.2	6.5
RPCC,4	**2.2**	**1.3**	7.7	2.4	**1.2**	9.6	**1.8**	**1.1**	**6.1**	**1.9**	**1.1**	**6.4**
HPPCC	2.8	1.4	10	3.2	1.5	13	3.6	1.8	14	3.9	1.9	15
Foveon												
PCC,1 (LCC)	3.6	2.5	10	3.9	3.2	11	2.5	1.6	7.5	2.7	1.8	8.0
PCC,2	4.0	3.1	10	4.8	2.6	18	2.6	1.8	7.2	2.6	1.7	8.5
PCC,3	3.6	2.7	11	4.9	1.8	16	2.5	1.9	7.2	2.6	1.5	9.6
PCC,4	2.6	2.1	7.1	5.7	1.6	22	2.2	1.6	5.9	3.3	1.5	13
LUT	4.5	2.9	15	4.0	2.5	12	2.9	2.2	7.9	3.1	1.9	11
RPCC,2	2.9	1.8	7.0	3.2	1.8	10	2.0	**1.4**	5.5	2.0	**1.4**	5.8
RPCC,3	**2.2**	**1.4**	**6.4**	**2.4**	1.6	**6.4**	**1.9**	**1.4**	5.0	**1.9**	**1.4**	**5.1**
RPCC,4	**2.2**	**1.4**	**6.4**	**2.4**	**1.5**	6.5	**1.9**	**1.4**	**4.9**	**1.9**	**1.4**	**5.1**
HPPCC	5.4	3.4	18	5.0	3.4	16	3.3	2.2	9.2	3.4	2.3	9.1

the DC dataset the RPCC performs worse than PCC, but for the smaller SG dataset the situation is reversed and for the largest and most relevant SFU dataset, the results are comparable for the Sony sensor and slightly favour PCC for the Foveon sensor. The LUT method provided the best results for the larger datasets for the Sony sensor. For the Foveon sensor, it performed less well, comparable to the PCC of the 2^{nd} or 3^{rd} degree.

2) Variable Exposure: Next, for the DC and SFU datasets, we simulated an increase and decrease in the scene radiance by multiplying camera responses and the ground truth XYZs by factors $\frac{1}{2}$ and 2. We used these corresponding sets of RGBs and XYZs to test the same colour correction models. The results of these simulations can be seen in Table III, which shows that the PCC (as well as LUT) models deteriorate under change of scene radiance/exposure condition, whereas the RPCC models remain invariant. An important observation is the fact that the RPCC results are always better than the results obtained for the LCC - the only polynomial model, which is invariant to the change of radiance or exposure. The message from Table III as well as Fig. 1 is clear. If you carry out naïve polynomial regression to fit data at different exposures, high error can result. Conversely, the RPCC works well independent of exposure. Further, the LUT interpolation exhibits the same drawback of the high-degree polynomials. Note that the entries in two columns called 'DC/SFU divided by 2' in Table III for the root-polynomial methods (as well as LCC and HPPCC) are as expected the same as the results for these methods in Table II. As to the other two columns called 'DC/SFU multiplied by 2', the results are slightly different as we took into account a smaller number of patches, which did not saturate at any of the three colour channels. The results in Table III also show that varying the exposure has a larger negative impact on the PCC and LUT models for the Foveon sensor than for the Sony.

The HPPCC method does not compare favourably with the RPCC. Reference [26] compared the results of HPPCC to the LCC and the PCC of degree two. The HPPCC outperformed both of them. Our results are more mixed. For the Sony sensor, the results of the SG and DC datasets in Table II (fixed exposure) confirm the results shown in [26] i.e. the HPPCC results are better than LCC and also better (or at least comparable) with PCC of degree 2. Here, we can also see that HPPCC is worse than polynomial models of higher degree and all the root-polynomials. However, this is no longer the case for the largest SFU dataset. The failure of HPPCC here comes from the fact that it uses only a small subset of 1995 samples to learn the colour correction matrices, whereas the other methods were trained using the leave-one-out procedure that uses 1994 samples. We also discovered that HPPCC is very sensitive to the selection of the training samples.

For the Foveon sensor, the HPPCC provides even worse results than the LCC. This is due to the broad shape of the sensors, that require a more "aggressive" colour correction. The fact that the responses are desaturated means they are located nearer the white point in the chromaticity space. The HPPCC is calculated in each hue slice based on only three patches: white and two certain chromatic patches. The fact that these two patches are relatively close to white means that the plane through these points is more difficult to determine.

3) Noise Influence: We also investigated the influence of the shot noise on the PCC and RPCC. A random noise with $\sigma = \sqrt{N}$, where N denotes a single channel value was added to each channel before transforming the patch with the colour correction matrix. We assumed the well

TABLE IV

AS IN TABLES II AND III (DC AND SFU DATASETS, SONY SENSOR), BUT WITH ADDITION OF THE SHOT NOISE. WELL CAPACITY SET TO 4000

dataset	DC			DC divided by 2			DC multiplied by 2		
model type ($N = 3$)	mean	med	95 pt.	mean	med	95 pt.	mean	med	95 pt.
PCC,1 (LCC)	5.4	4.2	14	6.5	5.1	17	5.2	3.2	22
PCC,2	4.6	3.6	12	6.7	5.7	16	4.9	3.5	15
PCC,3	4.2	**3.3**	9.2	6.2	5.1	14	4.3	3.0	18
PCC,4	**4.1**	3.6	**8.2**	6.2	5.3	14	4.0	2.9	**10**
RPCC,2	4.4	3.5	10	5.4	**4.5**	**11**	**3.7**	2.9	**10**
RPCC,3	4.4	**3.3**	11	**5.3**	**4.5**	**11**	3.8	**2.8**	11
RPCC,4	**4.1**	3.4	9.0	5.7	5.0	14	**3.7**	**2.8**	11
dataset	SFU			SFU divided by 2			SFU multiplied by 2		
PCC,1 (LCC)	4.5	3.6	10	5.5	4.8	12	4.0	2.8	10
PCC,2	4.3	3.5	9.8	5.6	4.8	12	3.7	2.9	9.2
PCC,3	4.0	3.5	9.0	5.6	5.0	12	3.8	2.9	10
PCC,4	3.9	3.4	**8.3**	5.6	4.9	12	3.7	2.8	11
RPCC,2	4.0	3.5	8.8	5.3	4.7	11	**3.3**	2.7	8.0
RPCC,3	**3.8**	**3.2**	8.5	5.2	4.7	11	**3.3**	2.7	7.9
RPCC,4	3.9	3.4	**8.3**	**5.0**	**4.5**	**10**	**3.2**	**2.6**	**7.5**

TABLE V

AS IN TABLES II AND IV (SFU DATASET, SONY SENSOR), BUT FOR THE ILLUMINANTS A AND F11

dataset	SFU			SFU (noise)			SFU div. by 2 (noise)			SFU mult. by 2 (noise)		
model type ($N = 3$)	mean	med	95 pt.	mean	med	95 pt.	mean	med	95 pt.	mean	med	95 pt.
Illuminant A												
PCC,1 (LCC)	3.6	2.0	12	5.5	4.2	13	6.8	5.5	16	5.1	3.4	14
PCC,2	3.4	2.0	11	5.5	4.2	14	7.0	5.9	16	4.6	3.3	13
PCC,3	2.7	1.5	9.0	4.7	3.8	12	6.5	5.4	15	4.7	3.3	15
PCC,4	**2.4**	1.5	8.5	**4.6**	3.9	**11**	6.8	5.6	16	4.6	3.2	15
RPCC,2	2.8	1.6	10	4.8	3.9	12	6.1	5.2	14	4.1	**3.0**	10
RPCC,3	2.5	1.6	8.7	**4.6**	3.8	**11**	**5.9**	**4.9**	**13**	**3.9**	**3.0**	10
RPCC,4	**2.4**	**1.4**	**8.0**	**4.6**	**3.7**	**11**	6.1	5.0	**13**	**3.9**	**3.0**	**9.7**
Illuminant F11												
PCC,1 (LCC)	1.7	0.8	6.1	3.7	3.0	8.3	4.8	4.2	11	3.0	2.3	7.5
PCC,2	1.7	1.0	5.7	3.6	3.0	8.5	4.9	4.4	10	3.0	2.4	7.2
PCC,3	1.4	0.8	5.1	3.5	3.0	7.9	4.8	4.2	10	3.1	2.4	8.3
PCC,4	**1.3**	**0.7**	4.6	3.4	3.0	7.3	4.8	4.2	10	3.0	2.2	8.3
RPCC,2	1.5	0.8	5.5	3.5	**2.9**	7.8	4.7	**4.1**	10	2.8	2.3	6.3
RPCC,3	**1.3**	0.8	5.0	3.4	3.0	7.7	**4.6**	**4.1**	10	**2.7**	2.3	6.4
RPCC,4	**1.3**	0.8	**4.5**	**3.3**	**2.9**	**7.0**	**4.6**	**4.1**	**9.5**	**2.7**	**2.1**	**6.2**

capacity [34] of 4000. Table IV contains the results of these simulations for DC and SFU datasets respectively. Having analysed the results in Tables I - III and keeping in mind the length of the tables, we did not test the LUT and HPPCC methods beyond the first two experiments.

Table IV results confirm our earlier observations. Of course, the colour correction performance deteriorates for all models when shot noise is added, but in general it is the RPCC which produces better or at least the results that are comparable with the best PCC. From the statistics of the shot noise, we know that decreasing the exposure that is equivalent to placing an object in a shadow will decrease SNR [35] and this is evident from the second column of Table IV, where the results are clearly worse than those in the first column. On the other hand, placing an object in a brighter light (Table IV, column three), increases SNR and hence both types of models improve. However then, the polynomial models are affected by the exposure change and this is the reason why they do not improve as much as the root-polynomials.

4) Additional Illuminants: We looked whether our results are not affected by the choice of the illuminant. Table V contains the results of the same experiments for illuminants A and F11 [18] for the SFU dataset.

The trends in results for these two illuminants are similar with an exception that colour correction is easier for the F11 illuminant i.e. the LCC provides results which are only slightly worse than any of the PCC or RPCC. The colour error for this illuminant is significantly smaller than for A and D65. This was to be expected as the F11 spectrum comprises distinctive peaks, which in some sense sample the reflectance spectra and hence decrease the variance of the colour signals. Two different reflectance spectra, which vary mostly at wavelengths where the F11 spectrum is low, will produce similar colour signals and hence similar both RGB and XYZ pairs. As a corollary, an illuminant comprising only three very narrow peaks would not require anything beyond the simple LCC, which would provide a perfect colour correction result.

V. Discussion

Noise is an important problem in colour correction as in general the process of colour correction boosts noise. The impact of noise on the PCC in particular is significant, which is the reason why the various versions of the LCC are more popular with the manufacturers. For example, the LCC can be optimized for different exposure levels so that for low exposure, a less "aggressive" colour correction is performed i.e. a suboptimal colour correction is an acceptable trade-off for improved noise variance; and for the high exposure, the colour transform matrix can become more "aggressive" i.e. a more optimal colour correction is performed as the noise variance is a smaller problem [27]. The same type of trade-off scheme could be employed for the root-polynomial and the polynomial methods. Moreover, there is no reason that would prevent us from mixing different types of transforms so e.g. the lowest exposure level could use the LCC, the middle exposure the RPCC optimized for a tolerable noise level for that exposure, and the high exposure could use the most "aggressive" RPCC or similar. While the RPCC will undoubtedly boost noise more than the LCC, its exposure invariance and low number of terms needed to achieve significant edge over the LCC would suggest that this polynomial type technique could play part in a scheme similar to the one described above.

Another interesting observation about the RPCC is that, the results obtained for different degrees are relatively similar, which is particularly true for the Sony sensor. Usually, the largest improvement over the linear model takes place in the second degree root-polynomial by adding just three extra terms into the model. The results of the third and the fourth degree RPCC are very similar and only slightly better than those of the second degree. In Table II, we can see that for the Sony sensor the 2^{nd} degree RPCC (6 terms) outperforms even 4^{th} degree PCC (34 terms) for the SG dataset and as to the other results, 3^{rd} degree RPCC (13 terms) is comparable to the best performing 4^{th} degree PCC (34 terms). Thus, the smaller number of terms of root-polynomials is their yet another advantage over the polynomials. This suggests that at least for the Sony sensor the shape of the underlying 3D mapping is well described by the low-degree root-polynomial basis. It is also notable that the improvement discussed is particularly visible in the smallest dataset (SG) leading to a conclusion that despite the use of the leave-one-out cross-validation, there is some over-fitting taking place. In that case, the lower dimensionality of the root-polynomial model will provide the smoother solution, which will be less prone to over-fitting.

A clue to the good performance of low in number set of root-polynomials may also lay in the nature of the non-linear RGB to XYZ mapping. From the low dimensional assumption of the reflectance spectra and a relatively good performance of the linear transform, we know that the mapping is approximately linear, thus we can expect that any non-linearities will be smooth across the sensor domain (the idea supported by e.g. the early work of Wandell and Farrell [36]) and therefore the non-linear alterations of the individual sensors with root-polynomials may suffice to model those non-linearities and in some cases they may model those non-linearities better than the polynomials. Note, the root-polynomial cross-term basis functions are different than the polynomial cross-terms, in particular they are smoother around the achromatic region (see the two bottom sub-figures in Fig. 4). The performance of the low-degree RPCC against the PCC will depend on the shape of the sensor sensitivities in question. We have seen in Table II that the improvement of root-polynomials over polynomials was more visible for the Sony sensor than for the Foveon.

It is worth noting that as intensity of the light/exposure deviates from the original, the failure of the PCC does not manifest itself in all the patches equally, but rather it can be observed in few patches. Thus, it is important to look at the 95 percentile error as well as the mean and the median, as it is there where we can see significant error increases i.e. the 95 percentile error increases faster than the mean error and even faster than the median. For example see Table I, where the 95 percentile errors for the 3^{rd} degree PCC in the 3 consecutive columns were 3.1; 9.7 and 23 and the corresponding median errors are 1.6; 1.9 and 2.5. These large error increases for the top 5% worst patches will result in easy to detect visual differences, as it is the differences of around $10\Delta E$, which are easy to spot visually. This observation is consistent with what we can see in Fig. 2, 3 and 5 where the colour correction errors can be spotted only for a relatively small number of colour chart patches.

On another note, one might observe that degree of one and hence the scene radiance/exposure invariance property of all root-polynomial terms can be also achieved by application of not only fractional powers, but also negative (not necessarily fractional) e.g. r^2g^{-1} or $r^{3/2}g^{-1/2}$. While this would indeed achieve the key property that we emphasised so much in this paper, it creates the problem at the low end of the sensor responses. As sensor responses tend to zero, the term containing the negative power becomes unstable. This effect makes the above approach inapplicable to our problem.

VI. Conclusions

'Root-Polynomial Colour Correction' builds on the earlier widely used polynomial models, but unlike its predecessors is invariant to the change of camera exposure and/or scene irradiance. The results presented in this paper show that this algorithm outperforms linear regression and offers a significant improvement over polynomial models when the exposure/scene irradiance varies. RPCC falls firmly into the well established family of linear and polynomial colour correction and therefore certain improvements to the last methods presented earlier in the literature (such as white-point preserving method) can be applied for RPCC case as well.

Acknowledgements

The authors' thanks go to Stuart Crichton for his help in acquiring hyperspectral images. They also thank Casper Andersen for explaining the details of the HPPCC algorithm.

REFERENCES

[1] G. Wyszecki and W. S. Stiles, *Color Science: Concepts and Methods, Quantitative Data and Formulae*. New York, NY, USA: Wiley, 1982.

[2] R. Luther, "Aus dem Gebiet der Farbreizmetrik," *Zeitschrift Tech. Phys.*, vol. 8, pp. 540–558, 1927.

[3] H. E. Ives, "The transformation of color-mixture equations from one system to another," *J. Franklin Inst.*, vol. 180, no. 6, pp. 673–701, Dec. 1915.

[4] B. A. Wandell, *Foundations of Vision*. Sunderland, MA, USA: Sinauer Associates, Inc., 1995.

[5] P. Green and L. MacDonald, Eds., *Colour Engineering: Achieving Device Independent Colour*. New York, NY, USA: Wiley, 2002.

[6] P.-C. Hung, "Colorimetric calibration in electronic imaging devices using a look-up-table model and interpolations," *J. Electron. Imag.*, vol. 2, no. 1, pp. 53–61, Jan. 1993.

[7] H. R. Kang, "Colour scanner calibration," *J. Imag. Sci. Technol.*, vol. 36, pp. 162–170, Mar./Apr. 1992.

[8] M. J. Vrhel, "Mathematical methods of color correction," Ph.D. dissertation, Dept. Elect. Comput. Eng., North Carolina State Univ., Raleigh, NC, USA, 1993.

[9] R. S. Berns and M. J. Shyu, "Colorimetric characterization of a desktop drum scanner using a spectral model," *J. Electron. Imag.*, vol. 4, no. 4, pp. 360–372, Oct. 1995.

[10] G. D. Finlayson and M. S. Drew, "Constrained least-squares regression in color spaces," *J. Electron. Imag.*, vol. 6, no. 4, pp. 484–493, 1997.

[11] G. Hong, M. R. Luo, and P. A. Rhodes, "A study of digital camera colorimetric characterization based on polynomial modeling," *Color Res. Appl.*, vol. 26, no. 1, pp. 76–84, Feb. 2001.

[12] T. L. V. Cheung and S. Westland, "Color camera characterisation using artificial neural networks," in *Proc. 10th Color Imag. Conf., Color Sci. Eng. Syst., Technol., Appl.*, vol. 4. 2002, pp. 117–20.

[13] S. H. Lim and A. Silverstein, "Spatially varying color correction matrices for reduced noise," Imaging Systems Lab., HP Lab., Palo Alto, CA, USA, Tech. Rep. HPL-2004-99, Jun. 2004.

[14] H. R. Kang and P. G. Anderson, "Neural network applications to the color scanner and printer calibrations," *J. Electron. Imag.*, vol. 1, pp. 125–135, Apr. 1992.

[15] L. Xinwu, "A new color correction model for based on BP neural network," *Adv. Inf. Sci. Service Sci.*, vol. 3, no. 5, pp. 72–78, Jun. 2011.

[16] J. Cohen, "Dependency of the spectral reflectance curves of the Munsell color chips," *Psychonomic Sci.*, vol. 1, nos. 1–2, pp. 369–370, Jan. 1964.

[17] D. H. Marimont and B. A. Wandell, "Linear models of surface and illuminant spectra," *J. Opt. Soc. Amer. A*, vol. 9, no. 11, pp. 1905–1913, Nov. 1992.

[18] R. W. G. Hunt and M. R. Pointer, *Measuring Colour*, 4th ed. New York, NY, USA: Wiley, 2011.

[19] K. Barnard, L. Martin, B. Funt, and A. Coath, "A data set for color research," *Color Res. Appl.*, vol. 27, no. 3, pp. 147–151, Jun. 2002.

[20] P. M. Hubel, "Foveon technology and the changing landscape of digital cameras," in *Proc. 13th Color Imag. Conf. (CIC)*, 2005, pp. 314–317.

[21] R. C. Aster, B. Borchers, and C. H. Thurber, *Parameter Estimation and Inverse Problems*, 2nd ed. Amsterdam, The Netherlands: Elsevier, 2013.

[22] G. Taubin and D. B. Cooper, "Object recognition based on moment (or algebraic) invariants," in *Geometric Invariance in Computer Vision*, J. L. Mundy and A. Zisserman, Eds. Cambridge, MA, USA: MIT Press, 1992, pp. 375–397.

[23] R. Stanley, *Enumerative Combinatorics*, vol. 1. Cambridge, U.K.: Cambridge Univ. Press, 2011.

[24] P. C. Hansen, *Rank-Deficient and Discrete Ill-Posed Problems: Numerical Aspects of Linear Inversion*. Philadelphia, PA, USA: SIAM, 1998.

[25] M. J. Vrhel and H. J. Trussell, "Color correction using principal components," *Color Res. Appl.*, vol. 17, no. 5, pp. 328–338, Oct. 1992.

[26] C. Andersen and J. Y. Hardeberg, "Colorimetric characterization of digital cameras preserving hue planes," in *Proc. 13th Color Imag. Conf. (CIC)*, Jan. 2005, pp. 141–146.

[27] U. Barnhoefer, J. M. DiCarlo, B. P. Olding, and B. A. Wandell, "Color estimation error trade-offs," *Proc. SPIE*, vol. 5017, pp. 263–273, May 2003.

[28] D. H. Brainard and W. T. Freeman, "Bayesian color constancy," *J. Opt. Soc. Amer. A*, vol. 14, no. 7, pp. 1393–1411, 1997.

[29] P. Royston and D. G. Altman, "Regression using fractional polynomials of continuous covariates: Parsimonious parametric modelling," *J. Roy. Statist. Soc. Ser. C (Appl. Statist.)*, vol. 43, no. 3, pp. 429–467, 1994.

[30] P. Royston and W. Sauerbrei, *Multivariable Model-Building*. New York, NY, USA: Wiley, 2008.

[31] G. E. P. Box and P. W. Tidwell, "Transformation of the independent variables," *Technometrics*, vol. 4, no. 4, pp. 531–550, 1962.

[32] E. Garcia, R. Arora, and M. R. Gupta, "Optimized regression for efficient function evaluation," *IEEE Trans. Image Process.*, vol. 21, no. 9, pp. 4128–4140, Sep. 2012.

[33] M. Mackiewicz, S. Crichton, S. Newsome, R. Gazerro, G. Finlayson, and A. Hurlbert, "Spectrally tunable LED illuminator for vision research," in *Proc. 6th Colour Graph., Imag. Vis. (CGIV)*, vol. 6. Amsterdam, The Netherlands, Apr. 2012, pp. 372–377.

[34] D. B. Murphy and M. W. Davidson, *Fundamentals of Light Microscopy and Electronic Imaging*. New York, NY, USA: Wiley, 2013.

[35] W. K. Pratt, *Digital Image Processing*, 4th ed. New York, NY, USA: Wiley, 2007.

[36] B. A. Wandell and J. E. Farrell, "Water into wine: Converting scanner RGB to tristimulus XYZ," *Proc. SPIE*, vol. 1909, pp. 92–101, Aug. 1993.

Graham D. Finlayson (M'15) is currently a Professor of Computing Sciences with the University of East Anglia. His research interests span color, physics-based computer vision, image processing, and the engineering required to embed technology in devices. Unusually, for an academic, his research is implemented in numerous commercial products ranging from standalone image enhancement software to the processing pipelines found in professional and mobile cameras and mobile phone cameras. He has authored over 250 refereed papers and co-authored 30 patents. He is a fellow of the Royal Photographic Society, the Society for Imaging Science and Technology, and the Institution for Engineering Technology. He was a recipient of the Philip Leverhilme Prize (2002) and the Royal Society-Wolfson Merit Award (2008). He received the Davies Medal for his contributions to the photographic industry from the Royal Photographic Society in 2009.

Michal Mackiewicz received the Ph.D. degree in computer science from the University of East Anglia (UEA), in 2007, and the M.Sc. degree in telecommunications from the University of Science and Technology, Krakow, in 2003. He is currently an Independent Research Fellow with UEA. His research interests include color perception, computer vision, image processing, and medical imaging.

Anya Hurlbert received the B.A. degree in physics from Princeton University, in 1980, the M.A. degree from Cambridge University, in 1982, the Ph.D. degree in brain and cognitive sciences from the Massachusetts Institute of Technology, in 1989, and the M.D. degree from the Harvard Medical School, in 1990. She trained as a Physicist, Physiologist, Neuroscientist, and Physician. She is currently a Professor of Visual Neuroscience and the Director of the Centre for Translational Systems Neuroscience with Newcastle University. Her main research interests are in understanding how the human visual system analyses and uses the information available in images, with a particular emphasis on the role of color in visual tasks, such as object recognition and material identification, and in translating these principles to machine vision. Her research interests also span in other applied areas, such as novel lighting technologies and the analysis of visual art.